Materials Science and Engineering A 387–389 (2004) 840–844

www.elsevier.com/locate/msea

Dislocation slip or deformation twinning: confining pressure makes a difference

Dong-Sheng Xu [a,*], Jin-Peng Chang [b], Ju Li [c], Rui Yang [a], Dong Li [a], Sidney Yip [b]

[a] *Titanium Alloy Laboratory, Institute of Metal Research, Chinese Academy of Sciences, 72 Wenhua Road, Shenyang 110016, China*
[b] *Department of Nuclear Engineering, Massachusetts Institute of Technology, 77 Massachusetts Ave., Cambridge, MA 02139, USA*
[c] *Department of Materials Science and Engineering, Ohio State University, 2041 College Road, Columbus, OH 43210, USA*

Received 25 August 2003; received in revised form 18 January 2004

Abstract

While b.c.c. metals deform plastically by dislocation motion or deformation twinning, the atomistic mechanisms governing the choice of deformation modes are not well established. Molecular dynamics simulations using the Finnis–Sinclair potential were carried out to explore the pressure dependence of the deformation response of b.c.c. molybdenum. The crystal was sheared in $(1\,1\,2)[\bar{1}\,\bar{1}\,1]$ under various confining pressures. The homogeneous nucleation stress of deformation twinning was found to increase with increasing confining pressure. Under sufficient pressure $(0\,1\,1)[\bar{1}\,\bar{1}\,1]$ dislocations were nucleated instead of twins. Details of the dislocation and twin nucleations were analyzed with the help of the multi-layer generalized stacking fault energies. A two-fault ($n = 2$) metastable twin state was found, in contrast to previous results using pair potentials.

Keywords: Twin; Nucleation; Molecular dynamics; b.c.c. metal; Mo; Pressure

1. Introduction

Dislocation glide and deformation twinning are the two major plastic deformation modes in metals and alloys. Their nucleation and multiplication/growth under stress govern the mechanical behavior of materials. Various models have been proposed for the nucleation of twin from dislocations [1–7]. But direct experimental confirmations of these models are rare. A measure of the "twinning tendency" at the crack tip of f.c.c. metals has recently been derived within the Peierls framework [8], which is still to be tested. Under extreme conditions such as shock-wave loading, the material deforms at very high strain rate and twinning may play an important role; however, large discrepancies exist with respect to the volume fraction of shock-induced twin, so the factors controlling twin nucleation are yet to be clearly identified [9]. In nanoindentation experiments, homogeneous nucleation of defects inside a perfect crystal can occur at extremely high stresses. A so-called Λ-criterion predicts the location and critical stress of homogeneous nucleation [10,11], by ascertaining when a local elastic wavelet starts to possess imaginary frequency and subsequently grows in amplitude. This criterion also provides some clues as to what kinds of defects may result after the instability. If the unstable elastic wave is longitudinal (sound wave), then a microcrack is likely to be nucleated. If the unstable elastic wave is transverse (shear wave), then a dislocation loop or twinning embryo may be nucleated. However, the atomistic details of this runaway dynamics are not yet clear. Also, it is noted that even in cases of shear wave instability, the nanoindentation setup induces a significant subsidiary pressure at the defect nucleation site (on the order of tens of GPa) in addition to the resolved shear stress, so it is important to study the influence of the confining pressure [19].

In this paper, nucleation and growth of deformation twins in b.c.c. Mo was simulated atomistically using the Finnis–Sinclair empirical potential [12]. Shear deformations were carried out under (initially) hydrostatic tension and compression to ascertain the effects of pressure. The atomic configurations of the homogeneously nucleated twin embryos were analyzed. Further interpretations were made

* Corresponding author. Tel.: +86 24 23971946; fax: +86 24 23891320.
E-mail address: dsxu@imr.ac.cn (D.-S. Xu).

0921-5093/$ – see front matter © 2004 Published by Elsevier B.V.
doi:10.1016/j.msea.2004.01.128

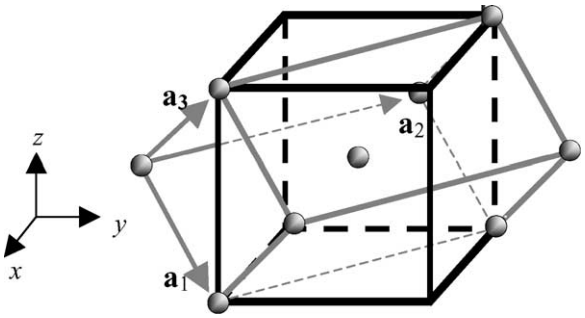

Fig. 1. Elementary cell with basis vectors $\mathbf{a}_1$, $\mathbf{a}_2$, $\mathbf{a}_3$ corresponding to vectors in the $[1\,1\,\bar{1}]$, $[\bar{1}\,1\,0]$ and $[1\,1\,1]$ directions, respectively. The b.c.c. unit cell is delineated by the thick lines. Twinning shear is along $-\mathbf{a}_1$ direction on the $\mathbf{a}_1 \times \mathbf{a}_2$ plane.

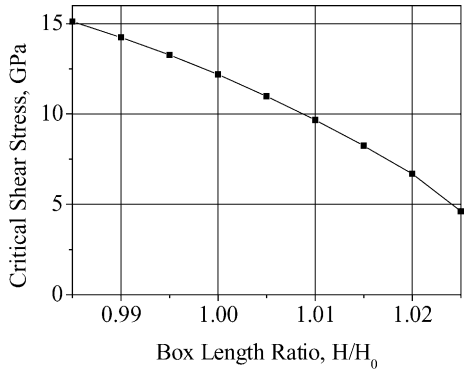

Fig. 2. Pressure dependence of the ideal shear strength in $(1\,1\,2)[\bar{1}\,\bar{1}\,1]$ (in the twining sense) at 1 K. H/H_0 is the ratio of the simulation box vector lengths to those at zero pressure. When $H/H_0 \leq 0.98$, $(0\,1\,1)[\bar{1}\,\bar{1}\,1]$ dislocation loops are nucleated instead of $(1\,1\,2)[\bar{1}\,\bar{1}\,1]$ twins.

by considering the static multi-layer generalized stacking fault energetics of a quasi 1D chain model.

2. Simulation method and setup

We perform molecular dynamics simulations at constant strain rate loading using the Finnis–Sinclair second-moment many body potential for molybdenum [12]. Simulation cells containing up to 0.5 million Mo atoms were employed in the calculations, with periodic boundary condition in all three directions. Shear displacements were imposed along $[\bar{1}\,\bar{1}\,1]$ direction on $(1\,1\,2)$ plane (both twinning and anti-twinning sense); the confining pressure being adjusted by changing the lattice parameter. Most of the simulations were carried out at very low temperatures (1 and 10 K), with temperature rescaling through a first-order feedback control scheme to remove the significant heat generated by plastic deformation. The shear strain rate ranged from 10^6 to $10^{10}\,s^{-1}$.

The simulation cell was chosen to be multiples of an elementary cell as shown in Fig. 1. The latter is spanned by $\mathbf{a}_1 = [1\,\bar{1}\,\bar{1}]a_0/2$, $\mathbf{a}_2 = [\bar{1}\,1\,0]a_0$ and $\mathbf{a}_3 = [1\,1\,1]a_0/2$ and contains two atoms. The twining plane $(1\,1\,2)$ is the plane spanned by $\mathbf{a}_1$ and $\mathbf{a}_2$. Twinning shear deformation is applied on the $(1\,1\,2)$ plane along the $[\bar{1}\,\bar{1}\,1]$ direction, i.e. $-\mathbf{a}_1$.

3. Results and discussion

3.1. Nucleation of twin and dislocation under confinement in b.c.c. Mo perfect crystal

At zero pressure, when the applied shear strain approached the ideal shear strain of the crystal, shear wave fluctuations became more and more localized. Finally a twin was nucleated in the perfect crystal sheared, via amplification and condensation of the shear waves of the lattice, in a manner similar to a four-stage scenario described previously [10,11]. The effect of pressure on the shear strength is shown in Fig. 2. The x-axis in this figure is the ratio of the simulation cell vector length to that under zero pressure, which is an indication of the confining pressure. The critical resolved shear stress (CRSS) for twinning shear on $(1\,1\,2)[\bar{1}\,\bar{1}\,1]$ increased with pressure increase from $P = -20$ to 12 GPa. Hydrostatic tension decreased the shear strength and yield strain of lattice. The increase of shear strength when the lattice was compressed can be understood as greater interactions when the atoms come into closer contact, thus making it more difficult for the crystal to deform. The yield strain is also different, from 11 to 6% depending on the confining pressure, with smaller values when the system was in tension. When a large enough hydrostatic pressure (e.g., 10 GPa) was applied, shearing the crystal along $(1\,1\,2)[\bar{1}\,1\,1]$ in the twining sense did not create a deformation twin, but instead nucleated a dislocation loop of $(0\,1\,1)[\bar{1}\,\bar{1}\,1]$ character, which has a positive Schmid factor with the applied shear stress.

The results of shearing in two opposite senses show that, under hydrostatic tension or small compression, for shear along $-\mathbf{a}_1$, twinning was favored, with CRSS at about 12 GPa at $P = 0$. The anti-twinning shear strength at $P = 0$ is about 14 GPa. The twinning/anti-twinning asymmetry observed was not as pronounced as predicted by density functional theory calculations, which gave an energy barrier for anti-twinning shear three times as large as that of twinning [13]. One reason is that $(0\,1\,1)[1\,1\,\bar{1}]$ dislocation was nucleated first in anti-twinning shear before stacking fault generation. This asymmetry is reflected in the asymmetric $(1\,1\,2)[\bar{1}\,\bar{1}\,1]$ energy profile on one-layer gamma surface [14,15]. In contrast, no such asymmetry exists for the gamma surface of the $(0\,1\,1)[\bar{1}\,\bar{1}\,1]$ slip system.

3.2. Yield behavior and atomic configuration of twinning under hydrostatic tension

The CRSS for twin nucleation decreased as the subsidiary tension increased. As can be seen in Fig. 3, when the cell was subjected to hydrostatic tension of 1%, the normal stress

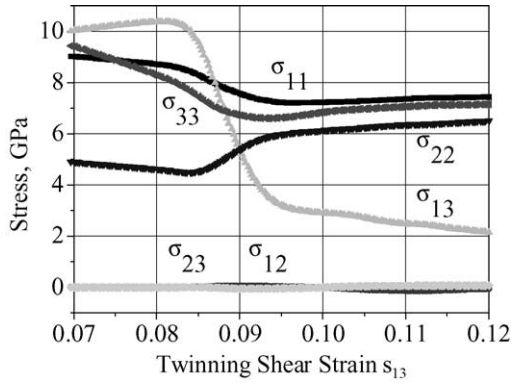

Fig. 3. Stress–strain curves for twinning shear under hydrostatic tension of 1%.

was around 9 GPa for σ_{11}, σ_{33} and 5 GPa for σ_{22}, the shear stress σ_{13} was about 10 GPa, before the twin nucleation. After the twin was nucleated, the normal stresses σ_{11} and σ_{33} dropped to about 7 GPa, while σ_{22} increased to about 6 GPa. This re-convergence of the normal stresses $\sigma_{11} \approx \sigma_{22} \approx \sigma_{33}$, which held exactly when the shear strain was zero, is due to the appearance of the twinned variant that has just the opposite shear strain–normal stress coupling with that of the original matrix, and also because σ_{13} itself has decreased.

It is commonly believed that deformation twinning can occur easily under high speed compression. However, our simulations show that twin is more easily formed by shearing under tension. There is experimental evidence that for Mo, deformation twinning occurs during tensile test and in bending specimen in the tension portion but not the compression portion [16]. Also, the density of twins increased with the distance from the origin of the crack, across the tensile face [16]. One can speculate that with the growth of the crack, the deformation rate around the crack tip increased and a mechanism with a high deformation rate, such as twinning, is needed to accommodate the plastic deformation. Deformation twin is also formed from the crack tip in atomistic simulation of f.c.c. Al, for certain crack configuration and lattice orientation when the sample was under tension [8].

The early stage of twin growth looks like a thin convex lens. It is thicker in the center and thinner around the edge, with each layer of stacking fault bounded by a ring of partial dislocation. Fig. 4 shows snapshots of a growing twin embryo. Due to the periodic boundary condition, the twin expanded and merged with its image to form a band composed of several layers of stacking faults. As deformation proceeds, this twinned band grows thicker and thicker by the formation of partial dislocation loops and their expansion on the twin boundary.

3.3. Yield behavior under compression

Under (initially) hydrostatic compression, say $H = 0.98H_0$, shearing on the same twinning system generated dislocation loop rather than twin. Analysis of the sheared

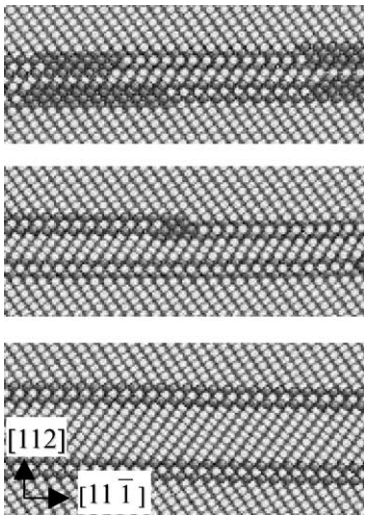

Fig. 4. Atomic configurations of the early stages of twin growth. These snapshots are side view from the $\mathbf{a}_2$ direction when sheared along $-\mathbf{a}_1$ axis. Darker atoms are those with wrong coordination number [17].

configurations showed that the slip system is $(0\,1\,1)[\bar{1}\,\bar{1}\,1]$. The change from deformation twinning to dislocation generation can be understood by an analysis of the multi-layer stacking fault energy profile as discussed below [15,18–20].

A small dislocation loop was formed at first as a partial loop enclosing a fault inside. The Burgers vector was about 2/3 of **b**, the Burgers vector of $\langle 1\,1\,1\rangle$ dislocation. When the loop expanded, the Burgers vector gradually grew into **b**. Some segments of the loop met and annihilated due to the periodic boundary condition. Because of the higher mobility of the edge and mixed portion of the dislocation loop, only the pure screw parts were eventually left in the crystal. In some simulations, even the screw segments may cross-slip and annihilate under the periodic boundary condition.

3.4. Multi-layer generalized stacking fault energy analysis

The competition between different modes of deformation can be studied with the aid of the multi-layer generalized stacking fault energy [15,18–20]. Here one uses a quasi 1D chain model, in which the deformation was conducted in a simplified and highly controlled manner. For the $(1\,1\,2)[\bar{1}\,\bar{1}\,1]$ twinning system, we let the atoms on each $(1\,1\,2)$ plane to move together like one atom, and ignore the large number of degrees of freedom within each plane. This way, there are only three degrees of freedom for each atomic layer. The simulation cell consisting of N layers of atoms therefore looks like a chain with N atoms. For our analysis, only the twinning shear is considered, while displacements in other directions are either fixed or allowed to relax. It has been verified that the effects of relaxation in other directions on the energetics are quite small [15]. The total energy of the system is a function of the relative displacement Δx_i of each layer i: $E(\Delta x_1, \Delta x_2, \ldots, \Delta x_i, \ldots, \Delta x_N)$. If relative shear occurs only between one pair of adjacent atomic

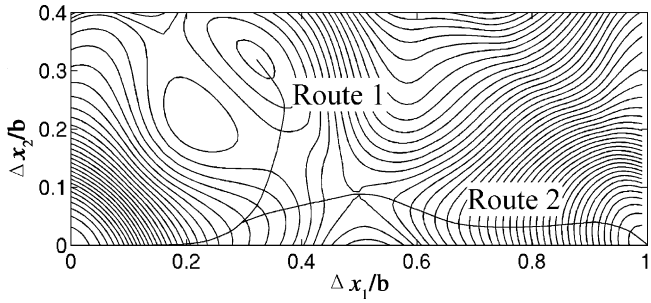

Fig. 5. Two-layer generalized stacking fault energy contour and minimum-energy path analysis for (1 1 2) [$\bar{1}\,\bar{1}$ 1] shear, with relaxations in directions perpendicular to [$\bar{1}\,\bar{1}$ 1]. The $\Delta x_1/b$, $\Delta x_2/b$ here are the normalized relative shear displacements. Route 1 turning up from the bifurcation point is a twinning route, leading to the final metastable state ($\Delta x_1 = \Delta x_2 = b/3$) which is an $n = 2$ twinning embryo, while route 2 leads to dislocation nucleation ($\Delta x_1 = b$, $\Delta x_2 = 0$).

layers, i.e., only one Δx_i is non-zero, a one-layer generalized stacking fault is formed, with the energy profile known conventionally as the γ-surface [18]. The γ-surface we have obtained is in agreement with previous calculations [15,18]. The easiest direction for shearing on the (1 1 2) plane is along [$\bar{1}\,\bar{1}$ 1]; any other shear faces a steeper energy barrier. There is no metastable energy minimum for one layer shear ($n = 1$) along the [$\bar{1}\,\bar{1}$ 1] direction on the (1 1 2) plane.

If three adjacent atomic planes are allowed to shear, two adjacent faults will form ($n = 2$). We can draw an energy contour map using Δx_1, Δx_2, the relative shear displacements of the two faults along [$\bar{1}\,\bar{1}$ 1] direction, as the axes. As shown in Fig. 5 [15], the lowest energy path in the two-layer stacking fault energy landscape is route 1, the upper route on the diagram. There is a metastable energy minimum at the end of route 1, which is a twin embryo. This is in contrast to the previous result of Vitek [18] using pair potentials, who found no metastable energy minimum for $n = 2$. We believe this is the first report of $n = 2$ metastable twin embryo in b.c.c. crystals, which needs to be confirmed by density functional theory calculations.

At zero pressure, the maximum energy barrier along route 1 is slightly lower than that along route 2 corresponding to the generation of a full dislocation, so one would predict that twinning should be favored. When the pressure is increased, the saddle free energy of route 1 rises faster than that of route 2. And when the two saddle free energies finally cross at about $P = 10$ GPa, a transition from twin nucleation to dislocation nucleation is predicted to occur.

Configurations corresponding to route 1 in Fig. 5 have been observed in our molecular dynamics simulations. As shown in Fig. 6, the first layer sheared to about $b/3$, then the 2nd layer started to shear. This corresponds to the upward turning from the bifurcation point in Fig. 5. Further layer shearing followed in a similar sequence. The twin structure here is $b/3$, $b/3$, $b/3$,... type, corresponding to a sharp twin boundary [18], or reflection twin boundary [20].

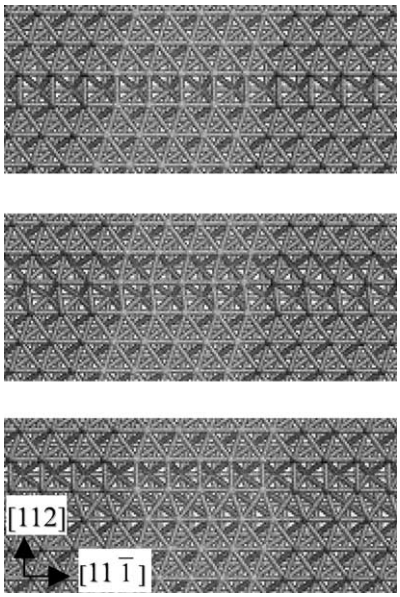

Fig. 6. Nucleation of deformation twin in a perfect lattice. Please note that only one layer shears at first, the 2nd layer starts to shear when the first layer stops at ~$b/3$. Nearest and next nearest neighbor bonds are shown [17].

4. Conclusions

Atomistic investigations of the pressure dependence of twin and dislocation nucleation behavior in perfect b.c.c. Mo are carried out using the Finnis–Sinclair interatomic potential. An energetic analysis based on the concept of multi-layer stacking faults is presented to elucidate the nucleation behavior. The following conclusions can be drawn:

(1) The confining pressure has an appreciable effect on defect nucleation behavior. Increase of pressure will not facilitate the nucleation of twin; instead, dislocation may be nucleated by shear in a twinning system. Hydrostatic tension promotes twin nucleation.
(2) The yield strength of twinning shear increases monotonically with increasing confining pressure.
(3) The twin nucleation behavior can be described with the aid of energetic analysis using the concept of multi-layer generalized stacking fault energy: nucleation follows the route with the lowest energy barrier and reaches a metastable free energy minimum.

Acknowledgements

The support from the Ministry of Science and Technology of China under grant TG2000067105 is gratefully acknowledged. D.S. Xu acknowledges support from K.C. Wong Fellowship for his visit to MIT.

References

[1] A.H. Cottrell, B.A. Bilby, Philos. Mag. 42 (1951) 573.
[2] A.W. Sleeswyk, Philos. Mag. 29 (1974) 407.
[3] S.G. Song, G.T. Gray, Philos. Mag. A 71 (1995) 661.
[4] K.P.D. Lagerlöf, in: M.H. Yoo, M. Wuttig (Eds.), Twinning in Advanced Materials, TMS, 1994, 75 pp.
[5] K.D.P. Lagerlöf, Acta Metall. Mater. 41 (1993) 2143.
[6] S. Mahajan, Acta Metall. 23 (1975) 671.
[7] J.W. Christian, S. Mahajan, Prog. Mater. Sci. 39 (1995) 1.
[8] E.B. Tadmor, S. Hai, J. Mech. Phys. Solids 51 (2003) 765.
[9] K. Wongwiwat, L.E. Murr, Mater. Sci. Eng. 35 (1978) 273.
[10] K.J. Van Vliet, J. Li, T. Zhu, S. Yip, S. Suresh, Phys. Rev. B 67 (2003) 104105.
[11] J. Li, K.J. Van Vliet, T. Zhu, S. Yip, S. Suresh, Nature 418 (2002) 307.
[12] M.W. Finnis, J.E. Sinclair, Philos. Mag. A 50 (1984) 45; M.W. Finnis, J.E. Sinclair, Philos. Mag. A 53 (1986) 161.
[13] A.T. Paxton, in: M.H. Yoo, M. Wuttig (Eds.), Twinning in Advanced Materials, TMS, 1994, 27 pp.
[14] M.S. Duesbery, V. Vitek, Acta Mater. 46 (1998) 1481.
[15] J.P. Chang, PhD Thesis, MIT, 2003.
[16] C.N. Reid, A. Gilbert, G.T. Hahn, Trans. Metall. Soc. AIME 236 (1966) 1024.
[17] J. Li, Model. Simul. Mater. Sci. Eng. 11 (2003) 173 (The software is available for free download at http://alum.mit.edu/www/liju99/Graphics/A/).
[18] V. Vitek, Scripta Metall. 4 (1970) 725.
[19] S. Ogata, J. Li, S. Yip, Science 298 (2002) 807.
[20] V. Paidar, Philos. Mag. A 48 (1983) 231.